Alvarez, R.; Bernet, S.; Lindenmueller, L.; Filsecker, F., "Characterization of a new 4.5 kV press pack SPT+ IGBT in Voltage Source Converters with clamp circuit," *Industrial Technology (ICIT), 2010 IEEE International Conference on*, pp.702-709, 14-17 March 2010

Characterization of a New 4.5 kV Press Pack SPT+ IGBT in Voltage Source Converters with Clamp Circuit

Rodrigo Alvarez, Steffen Bernet, Lars Lindenmueller and Felipe Filsecker
Power Electronics Lab
Technical University of Dresden
Dresden, Germany

Abstract—**Recently developed IGBT press pack devices have become a competition for IGCTs in high power industrial applications. This paper presents an overview of state-of-the-art medium voltage power semiconductors with active turn-off capability. A new 85 mm, 4.5 kV, 1.2 kA press pack SPT+ IGBT and the corresponding freewheeling diode are characterized for an operation in Voltage Source Converters. To reduce the IGBT turn-on losses compared to hard switching the clamp circuit configuration of IGCTs was adapted to the operation of press pack IGBTs. The switching behavior of IGBT and diode are characterized for varying dc-link voltages, load currents, junction temperatures and clamp inductances.**

I. Introduction

Recent technology developments of 3.3 kV, 4.5 kV and 6.5 kV IGBTs and IGCTs enabled a substantial improvement of medium voltage converters during the last years [1]–[3]. While medium voltage IGBT modules dominate in traction converters, IGCT press pack devices are mainly used in high power industrial applications, due to advantageous features of press pack cases compared to modules, like a higher thermal and power cycling capability and an explosion-free failure mode [4], [5].

However, recently developed press pack IGBT devices combine the advantages of IGBTs with those of press pack cases. Thus, press pack IGBTs have become a competition for IGCTs in medium and high power industrial applications like medium voltage drives (MVD).

Several authors have compared IGBTs on the basis of the technologies Field Stop (FS), Injection-Enhanced Gate Transistor (IEGT) and Soft Punch Through (SPT and SPT+) technology for hard and soft switching [6]–[10]. The SPT+ technology realizes low losses, smooth switching waveforms, a switching-self-clamping-mode and wide SOA limits [8], [9]. The new Westcode SPT+ IGBT press pack combines the advantages of the SPT+ IGBT technology with the advantages of press pack housing. The investigation of the 85 mm, 4.5 kV, 1.2 kA press pack SPT+ IGBT and the corresponding freewheeling diode at hard switching showed that the device is attractive for Medium Voltage Converters (MVC) [10]. It should be considered that two major manufacturers (TMEIC and Converteam) offer MVCs on the basis of hard switching press pack IGBTs. However, especially the substantially higher turn-on losses compared to IGCTs are a severe disadvantage which limits the silicon utilization of these devices [10].

To overcome this disadvantage, this paper considers an operation of IGBT and diode in Voltage Source Converters (VSCs) with clamp circuit. Thus the IGCT clamp circuit configuration is adapted to the operation of the 85 mm, 4.5 kV, 1.2 kA press pack IGBT. Finally the switching behavior of IGBT and diode are characterized for the first time in this circuit configuration for varying load currents, junction temperatures and clamp inductances. A comparison of the switching losses at hard switching and clamp operation shows a substantial reduction of the turn-on losses at clamp operation while the turn-off losses do not change remarkably.

II. Overview of MV power semiconductors

Maximum nominal voltage and current ratings of available power semiconductors with turn-off capability are shown in Fig. 1. Both commercially available IGBT modules and asymmetrical IGCTs achieve maximum device voltages of 6.5 kV. So far press pack IGBTs feature maximum device blocking voltages of 4.5 kV. It is interesting to note that the maximum turn-off current of the 125 mm, 4.5 kV, 2.4 kA press pack IGBT ($I_{C,M}$ = 4.8 kA) is slightly lower than that of the largest currently available 91 mm, 4.5 kV IGCT (I_{TGQM} = 5.5 kA). However, compared to the IGCT, the press pack IGBT features several advantages, like short circuit current limitation, short circuit turn-off capability, an adjustment of the switching behavior by the gate unit and a simpler device parallel and series connection. Obviously these characteristics simplify the converter design substantially [1]. A detailed overview of the state-of-the-art of medium voltage drives and power semiconductors has been presented in [5], [10].

III. Semiconductor Data and Test-bench

The 85 mm, 4.5 kV press pack IGBT T1200EB45E (Westcode), the commercially available gate unit C0030BG400 (Westcode) and the widely distributed 68 mm, 4.5 kV press pack diode D1031SH45T (Infineon) have been selected for the characterization of the devices. The minimum recommended gate resistance values have been used since the clamp circuit determines the IGBT turn-on and diode turn-off behavior compared

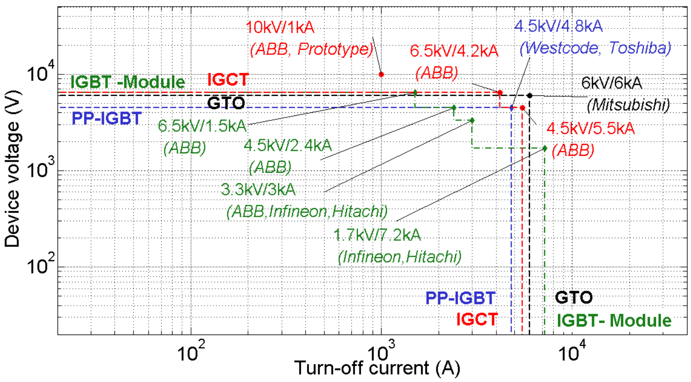

Fig. 1: Blocking voltage and maximum turn-off currents of state-of-the-art IGBTs and asymmetrical IGCTs.

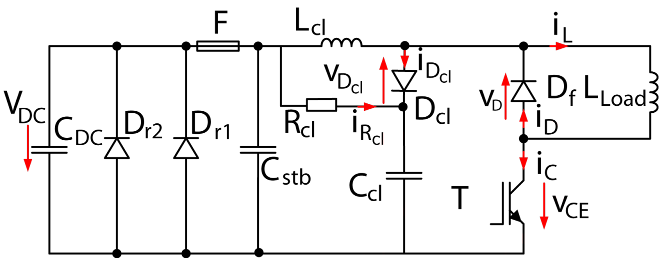

Fig. 2: Test circuit (C_{DC} = 4.5 mF, C_{stb} = 220 µF, C_{cl} = 10 µF, R_{cl} = 0.5 Ω, L_{cl} = 1 . . . 5.6 µH, L_{Load} = 1 mH)

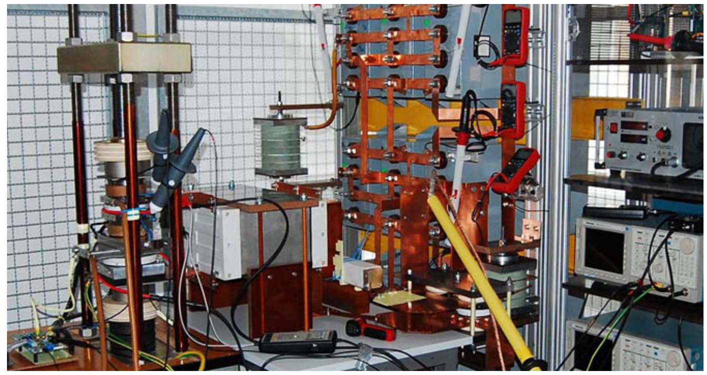

Fig. 3: IGBT press pack test bench

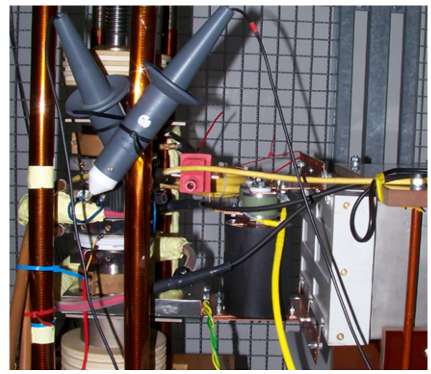

Fig. 4: IGBT Stack

TABLE I: Data of PP-IGBT, diode and gate unit

PP-IGBT Westcode T1200EB45E		PP-Diode Infineon D1031SH45T		Gate Unit Westcode C0030BG400		Clamp-Diode Infineon D1031SH45T	
V_{CES}	4.5 kV	V_{RRM}	4.5 kV	$V_{G,on/off}$	±15 V	V_{RRM}	4.5 kV
$V_{DC\text{-}link}$	2.8 kV	I_{FRMSM}	2.3 kA	$R_{G,on}$	3.3 Ω	I_{FRMSM}	2.3 kA
$I_{C(DC)}$	2.1 kA	I_{FAVM}	1.5 kA	$R_{G,off}$	2.2 Ω	I_{FAVM}	1.5 kA
$I_{C(nom)}$	1.2 kA	I_{RRM}	1.5 kA	P_o	12 W	I_{RRM}	1.5 kA

TABLE II: Data of test-bench and parameter variations

C_{DC}	4.5 mF	V_{DC}	2, 2.5 kV
C_{stb}	220 µF	i_L	100. . . 1800 A
L_{Load}	1 mH	T_j	25, 60, 90, 125 °C
R_{cl}	0.5 Ω	$R_{G,on}$	3.3 Ω
C_{cl}	10 µF	$R_{G,off}$	2.2 Ω
L_{cl}	1 , 2 and 5.6 µH		

to hard switching. Important data of power semiconductors and gate unit are summarized in Table I.

A buck converter was chosen as test circuit configuration for the investigation of the devices (Fig. 2 to 4). The clamp circuit consists of inductor, diode, capacitor and resistor (e.g. [3], [5], [11], [12]). Clamp inductor values of L_{cl} =1 µH, 2 µH and 5.6 µH have been selected to investigate the IGBT and freewheeling diode behavior at different rates of current change during natural commutations. The values of clamp capacitor and clamp resistance have been determined to enable a safe turn-off of the clamp diode, a short demagnetization time (less than 20 µs) of the clamp inductance and a limitation of the maximum IGBT voltage to v_{CE} =4.5 kV in the case of short circuits (Table II) [11]. The pressure distribution of the stack was the reason therefore, that the clamp diode was realized by the same diode type like the freewheeling diode (68 mm, 4.5 kV press pack diode D1031SH45T (Infineon) [11]).

A robust mechanical design was realized by 2 mm thick copper plates as connections between the dc-link capacitor C_{DC} and the stabilization capacitor C_{stb}. Thus the mechanical construction of the test bench is able to withstand short circuit currents of about 200 kA in case of an IGBT failure. However, the clamp inductance (L_{cl}) reduces the maximum value of failure short circuit currents to about 30 to 50 kA. The two diodes (D_{r1}, D_{r2}) and the fuse F are important components of the protection concept in case of an IGBT failure. The fuse prevents the dc-link capacitors from discharging completely through the stack, and the diodes (D_{r1}, D_{r2}) limit possible negative voltages across the dc-link capacitor preventing an oscillation of the failure short circuit current. The double pulse operation of the buck converter is the reason therefore, that the device junction temperatures can be adjusted by two heaters, which control the case temperatures [12]. The dc-link capacitor is charged by a high voltage power supply before the measurements are started. The variation of several measurement parameters, as depicted in Table II, cause about 500 measurements to characterize the switching behavior of IGBT and diode. Thus, a partially automated measurement system was used. The values of V_{DC}

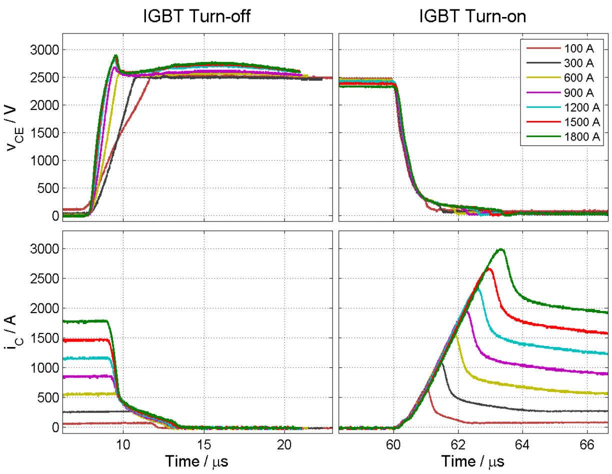

Fig. 5: IGBT switching waveforms for different collector currents for one set of parameters ($Tj = 125\,°C$, $V_{DC} = 2.5\,kV$ and $L_{cl\text{-}2} = 2\,\mu H$).

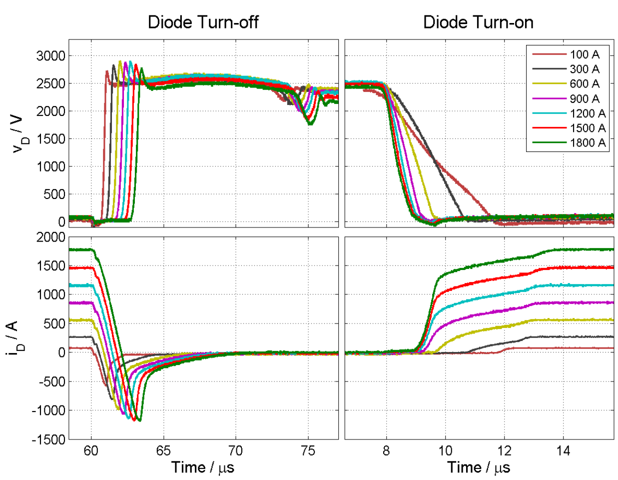

Fig. 6: Diode switching waveforms for different collector currents for one set of parameters ($Tj = 125\,°C$, $V_{DC} = 2.5\,kV$ and $L_{cl\text{-}2} = 2\,\mu H$).

and i_L are set through a LabVIEW graphical user interface in a computer connected to the test bench by a fiber optic cable. The storage and analysis of the data is carried out on a separate PC.

IV. Experimental Results

This section presents an overview of the experimental results. Three clamp configurations have been defined:

- Clamp 1 with $L_{cl\text{-}1} = 1\,\mu H$
- Clamp 2 with $L_{cl\text{-}2} = 2\,\mu H$
- Clamp 3 with $L_{cl\text{-}3} = 5.6\,\mu H$

For every set of temperature, dc-link voltage and clamp configuration, the switching behavior of IGBT and diode are investigated for seven different collector currents. Figs. 5 and 6 show exemplary measurements of the IGBT and diode switching behavior at $Tj = 125\,°C$, $V_{DC} = 2.5\,kV$ and clamp 2.

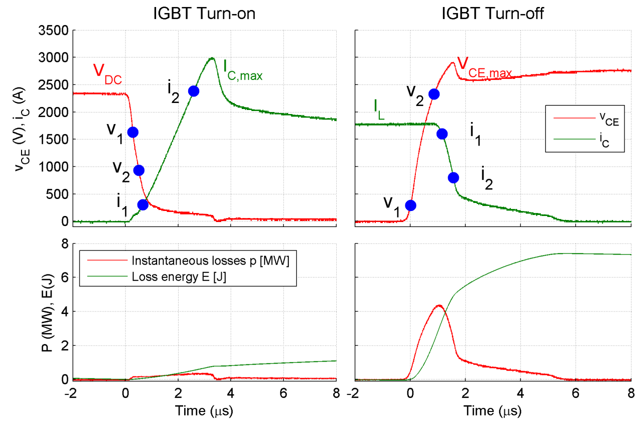

Fig. 7: Definitions of IGBT voltages and currents for calculations of dv/dt, di/dt and switching losses ($Tj = 125\,°C$, $V_{DC} = 2.5\,kV$, $i_C = 1.8\,kA$ and $L_{cl\text{-}1} = 1\,\mu H$).

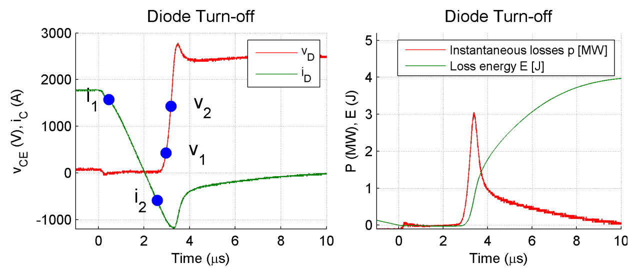

Fig. 8: Definitions of diode voltages and currents for calculations of dv/dt, di/dt and switching losses ($Tj = 125\,°C$, $V_{DC} = 2.5\,kV$, $i_C = 1.8\,kA$ and $L_{cl\text{-}1} = 1\,\mu H$).

TABLE III: Definition of voltage and current values for dx/dt calculations

		v1	v2	i1	i2
IGBT	on	$0.7V_{DC}$	$0.4V_{DC}$	$0.1I_{C,max}$	$0.8I_{C,max}$
	off	$0.1V_{DC}$	$0.8V_{DC}$	$0.9I_L$	$0.45I_L$
Diode	off	$0.15V_{DC}$	$0.5V_{DC}$	$0.9I_L + 0.1I_{rrm}$	$0.8I_{rrm} + 0.2I_L$

A. Parameter Definitions

The following variables have been used to analyze the switching behavior of IGBT and diode:

- V_{DC}, I_L : DC voltage and load current (constant during the commutation)
- $I_{C,max}$: Maximum IGBT current value during turn-on transients
- $V_{CE,max}$: Maximum IGBT voltage value during turn-off transients
- I_{rrm} : Peak reverse recovery current

Definitions of device voltages and currents to calculate rates of change are shown in Figs. 7 and 8, and Table III.

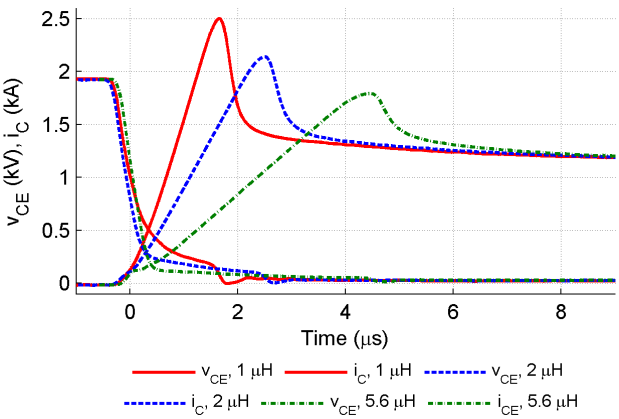

Fig. 9: IGBT turn-on transients at different clamp configurations ($T\text{j} = 125\,°\text{C}$, $V_{\text{DC}} = 2.5\,\text{kV}$ and $i_{\text{C}} = 1.2\,\text{kA}$).

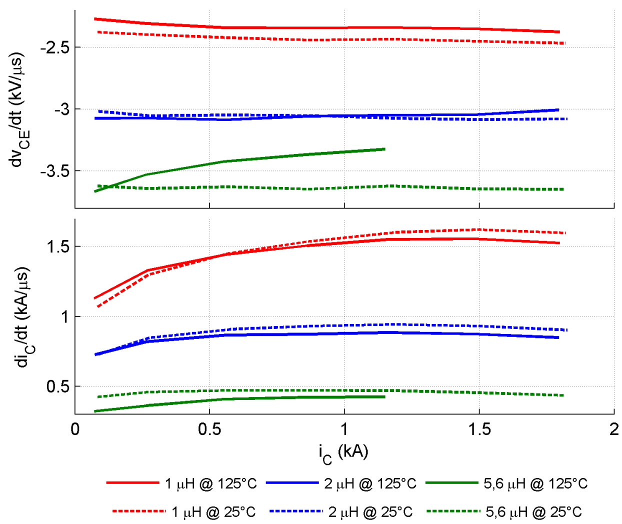

Fig. 10: IGBT turn-on $\text{d}i_{\text{C}}/\text{d}t$ and $\text{d}v_{\text{CE}}/\text{d}t$ at different clamp configurations ($T\text{j} = 25$ and $125\,°\text{C}$ and $V_{\text{DC}} = 2.5\,\text{kV}$).

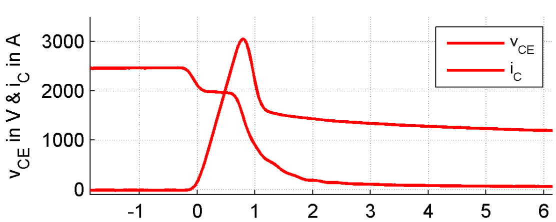

Fig. 11: IGBT turn-on at hard switching ($T\text{j} = 125\,°\text{C}$, $V_{\text{DC}} = 2.5\,\text{kV}$, $i_{\text{C}} = 1.2\,\text{kA}$, $L_{\sigma 1} = 120\,\text{nH}$, $\text{d}i_{\text{C}}/\text{d}t = 4\,\text{kA/μs}$, $E_{\text{on,IGBT}} = 4\,\text{J}$) [10].

The voltage and current slopes are defined as follows:

$$\frac{\text{d}i}{\text{d}t} = \frac{i_2 - i_1}{t(i_2) - t(i_1)} \tag{1}$$

$$\frac{\text{d}v}{\text{d}t} = \frac{v_2 - v_1}{t(v_2) - t(v_1)} \tag{2}$$

B. Influence of Clamp

Both IGBT and diode switching behavior are determined by the design of the clamp configuration. IGBT turn-on transients for different clamp inductance values can be seen in Fig. 9 for ($T\text{j} = 125\,°\text{C}$, $V_{\text{DC}} = 2.5\,\text{kV}$ and $i_{\text{C}} = 1.2\,\text{kA}$). It is obvious that an increase of the clamp inductance decreases the rate of current rise and increases the rate of voltage fall. Fig. 10 shows that the $\text{d}i_{\text{C}}/\text{d}t$ changes from $1.5\,\text{kA}/\mu\text{s}$ for $L_{\text{cl-1}}$ to $0.45\,\text{kA}/\mu\text{s}$ for $L_{\text{cl-3}}$ at the nominal current i_{C}. The inverse effect can be observed for the rate of voltage change $\text{d}v_{\text{CE}}/\text{d}t$, which changes from -2.3 kV/μs for $L_{\text{cl-1}}$ to -3.6 kV/μs for $L_{\text{cl-3}}$.

Fig. 11 shows the switching behavior of the hard switching IGBT [10]. It is important to note that both stress and losses of the hard switching IGBT are substantially higher. On the other hand the turn-on time at hard switching is smaller (about 3 μs for hard switching (HS) versus 8 μs for $L_{\text{cl-3}}$).

Figs. 12 and 13 show the corresponding waveforms and slopes for the turn-off transients of the freewheeling diode. The reduced rate of diode current fall (with increasing L_{cl}) causes smaller peak reverse recovery currents. Furthermore the reverse recovery current fall intervals decrease with increasing L_{cl}, causing lower overvoltage peaks during the diode turn-off. A snappy behavior of the diode has not been observed in the entire operating range.

Fig. 14 shows the corresponding switching diode behavior at hard switching [10]. The higher $\text{d}i_{\text{C}}/\text{d}t$ generates a larger peak reverse recovery current as well as increased stress and losses in the diode.

Figs 15 and 16 show the waveforms and slopes of IGBT turn-off transients for the different clamp configurations. Due to a constant clamp stray inductance the IGBT turn-off transients only slightly vary for different clamp inductance values. The only remarkable difference between the turn-off transients is the small increase of the overvoltage toward the end of the tail current caused by the demagnetization of L_{cl}. It is interesting that the influence of the junction temperature on the variation of rates of current and voltage changes is larger than that of different clamp inductance values.

The corresponding turn-off transient at hard switching is depicted in Fig. 17. A comparison to Fig. 15 shows that the switching behavior is almost the same for hard switching and clamp operation. The clamp operation generates slightly higher losses due to the overvoltage caused by the demagnetization of L_{cl}.

C. Switching Losses

The losses of IGBT, diode, clamp diode and clamp resistor are summarized by (3) (total semiconductor losses $E_{\text{Total SC}}$) and (4) (total losses E_{Total}) respectively.

$$E_{\text{Total SC}} = E_{\text{on,IGBT}} + E_{\text{off,IGBT}} + E_{\text{off,Diode}} \tag{3}$$

$$E_{\text{Total}} = E_{\text{Total SC}} + E_{\text{D},L_{\text{cl}}} + E_{\text{R},L_{\text{cl}}} \tag{4}$$

with

- $E_{\text{on,IGBT}}$: IGBT turn-on switching losses

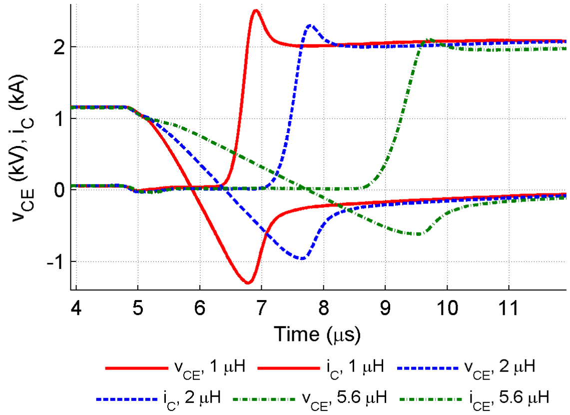

Fig. 12: Diode turn-off transients at different clamp configurations ($T\mathrm{j} = 125\,°\mathrm{C}$, $V_{\mathrm{DC}} = 2.5\,\mathrm{kV}$ and $i_{\mathrm{C}} = 1.2\,\mathrm{kA}$).

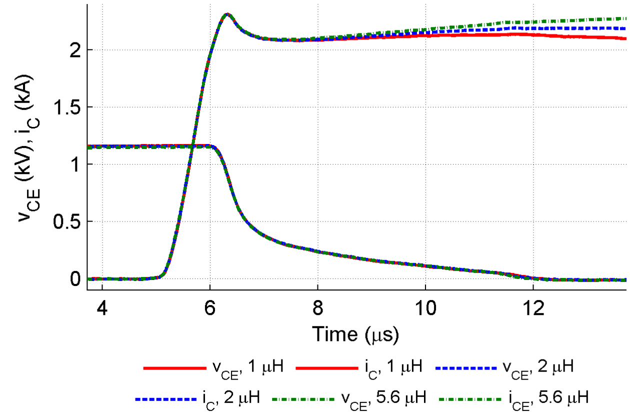

Fig. 15: IGBT turn-off transients at different clamp configurations ($T\mathrm{j} = 125\,°\mathrm{C}$, $V_{\mathrm{DC}} = 2.5\,\mathrm{kV}$ and $i_{\mathrm{C}} = 1.2\,\mathrm{kA}$).

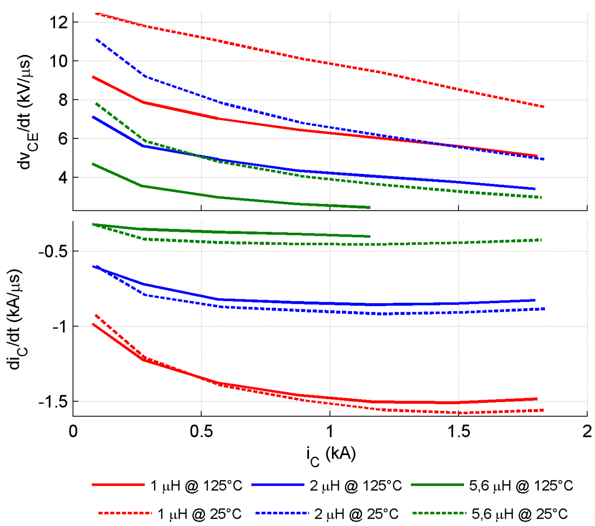

Fig. 13: Diode turn-off $\mathrm{d}i_{\mathrm{D}}/\mathrm{d}t$ and $\mathrm{d}v_{\mathrm{D}}/\mathrm{d}t$ at different clamp configurations ($T\mathrm{j} = 25$ and $125\,°\mathrm{C}$ and $V_{\mathrm{DC}} = 2.5\,\mathrm{kV}$).

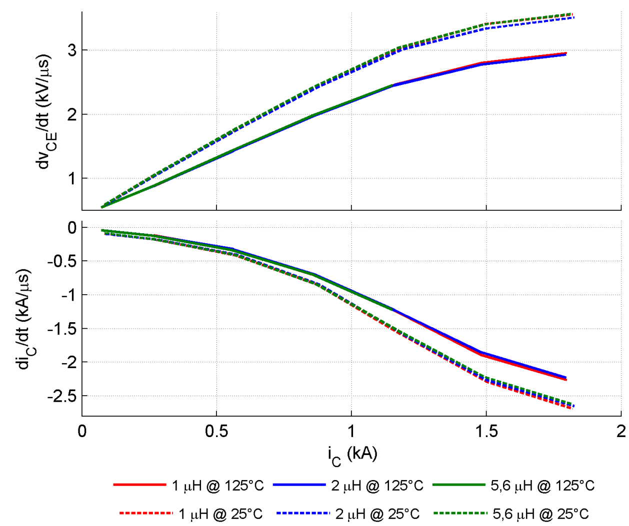

Fig. 16: IGBT turn-off $\mathrm{d}i_{\mathrm{C}}/\mathrm{d}t$ and $\mathrm{d}v_{\mathrm{CE}}/\mathrm{d}t$ at different clamp configurations ($T\mathrm{j} = 25$ and $125\,°\mathrm{C}$ and $V_{\mathrm{DC}} = 2.5\,\mathrm{kV}$).

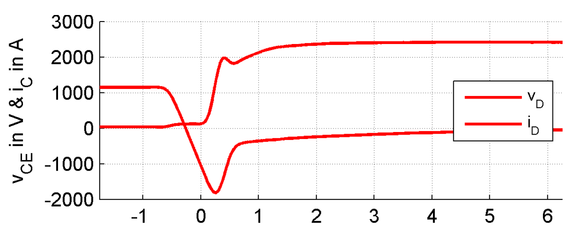

Fig. 14: Diode turn-off at hard switching ($T\mathrm{j} = 125\,°\mathrm{C}$, $V_{\mathrm{DC}} = 2.5\,\mathrm{kV}$, $i_{\mathrm{C}} = 1.2\,\mathrm{kA}$, $L_{\sigma 1} = 120\,\mathrm{nH}$, $\mathrm{d}i_{\mathrm{C}}/\mathrm{d}t$ = -4 kA/µs, $E_{\mathrm{off,Diode}} = 3.2\,\mathrm{J}$) [10].

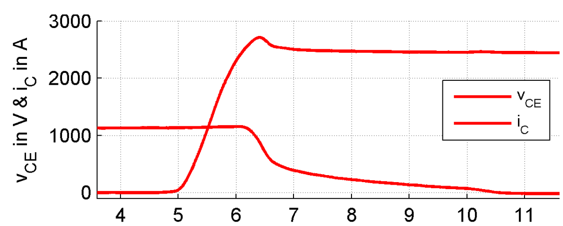

Fig. 17: IGBT turn-off at hard switching ($T\mathrm{j} = 125\,°\mathrm{C}$, $V_{\mathrm{DC}} = 2.5\,\mathrm{kV}$, $i_{\mathrm{C}} = 1.2\,\mathrm{kA}$, $L_{\sigma 1} = 120\,\mathrm{nH}$, $\mathrm{d}i_{\mathrm{C}}/\mathrm{d}t$ = -1.55 kA/µs, $E_{\mathrm{off,IGBT}} = 5\,\mathrm{J}$) [10].

- $E_{\mathrm{off,IGBT}}$: IGBT turn-off switching losses
- $E_{\mathrm{off,Diode}}$: Diode turn-off switching losses
- $E_{\mathrm{D},L_{\mathrm{cl}}}$: Losses of clamp diode
- $E_{\mathrm{R},L_{\mathrm{cl}}}$: Losses of clamp resistance

1) Semiconductor Losses: The influence of the different clamp configurations on the IGBT and diode switching losses for $T\mathrm{j} = 125\,°\mathrm{C}$ and $V_{\mathrm{DC}} = 2.5\,\mathrm{kV}$ are depicted in Fig. 18. The losses of clamp resistor and diode for the three presented clamp configurations at the same operating point can be seen in Fig. 22

The IGBT turn-on losses are drastically reduced (by about $90\,\%$) compared to hard switching. Obviously the IGBT turn-on

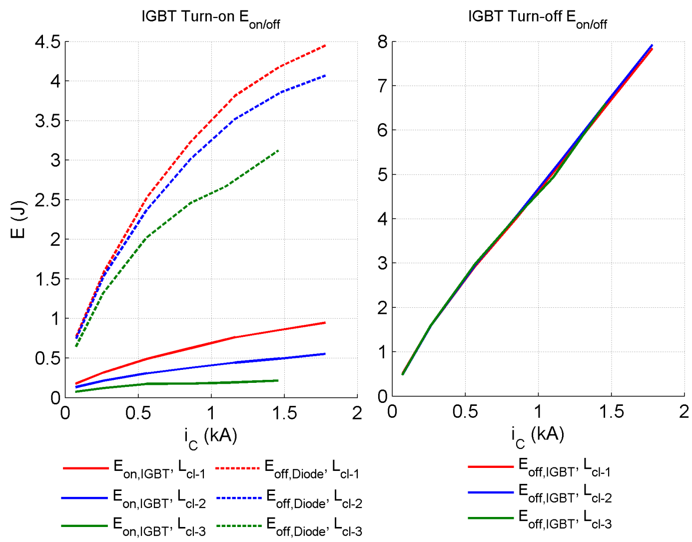

Fig. 18: Semiconductor losses as function of i_C current for different clamp configurations ($Tj = 125\,°C$, $V_{DC} = 2.5\,kV$).

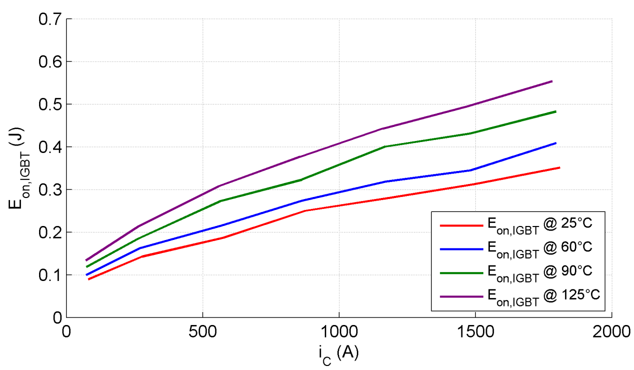

Fig. 19: IGBT turn-on losses as function of collector current i_C with Tj as parameter ($V_{DC} = 2.5\,kV$ and $L_{cl\text{-}2} = 2\,\mu H$).

losses increase for smaller L_{cl} values. Exemplarily the turn-on losses at nominal current increase from 0.25 J for $L_{cl\text{-}3} = 5.6\,\mu H$ to 0.32 J for $L_{cl\text{-}1} = 1\,\mu H$. The diode turn-off losses present a similar dependence on L_{cl} values since a reduction of di_D/dt causes lower reverse recovery currents and thus lower losses. Here the turn-off losses at nominal current change from 0.52 J for $L_{cl\text{-}3}$ to 0.84 J for $L_{cl\text{-}1}$. For $L_{cl\text{-}3}$ the losses are reduced about 70 % compared to hard switching. For IGBT turn-off transients the different clamp configurations cause only a slight change of the turn-off waveforms and losses (Fig. 18). It is interesting to note that these losses do not vary significantly from the losses at hard switching.

The dependence on the temperature of IGBT turn-on, diode turn-off and IGBT turn-off losses are shown in Figs. 19 to 21 for $V_{DC} = 2.5\,kV$ and $L_{cl\text{-}2}$.

The IGBT turn-on losses increase almost linear with the rising collector current between 0.19 mJ/A at 25 °C and 0.32 mJ/A at 125 °C. The losses at nominal current $i_C = 1.2\,kA$ increase by about 64 % from 25 °C to 125 °C (0.25 J to 0.41 J) (Fig. 19).

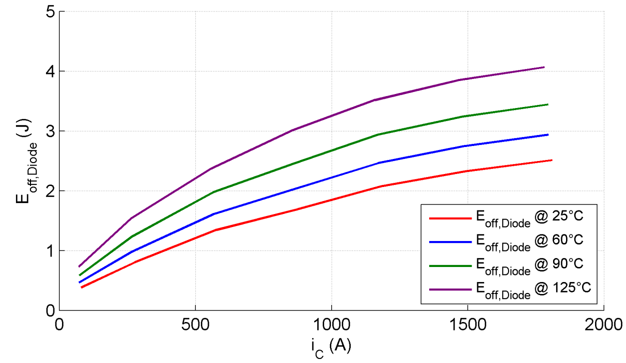

Fig. 20: Diode turn-off losses as function of collector current i_C with Tj as parameter ($V_{DC} = 2.5\,kV$ and $L_{cl\text{-}2} = 2\,\mu H$).

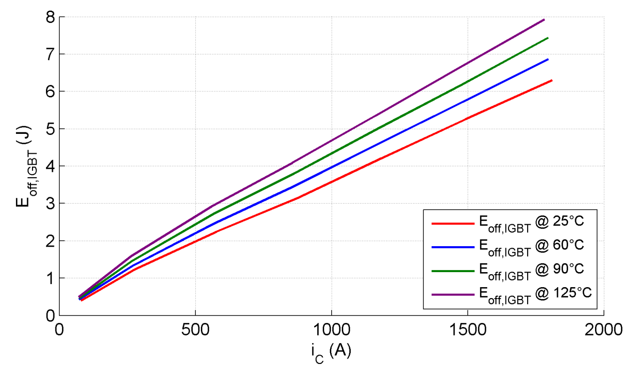

Fig. 21: IGBT turn-off losses as function of collector current i_C with Tj as parameter ($V_{DC} = 2.5\,kV$ and $L_{cl\text{-}2} = 2\,\mu H$).

The function of diode turn-off losses and device current is non linear. At nominal current the diode turn-off losses increase by about 42 % from 25 °C to 125 °C (2.09 J to 3.56 J). If the losses are linearized the slopes of the loss functions are in a range between 1.59 mJ/A at 25 °C and 2.68 mJ/A at 125 °C (Fig. 20).

The IGBT turn-off losses depend linearly on the collector current between 3.51 mJ/A at 25 °C and 4.46 mJ/A at 125 °C. The turn-off losses at nominal current rise by about 22 % from 25 °C to 125 °C (4.27 J to 5.51 J) for the $L_{cl\text{-}2}$ configuration (Fig. 21).

2) Clamp Losses: The clamp circuit produces losses in the diode D_{cl}, the resistance R_{cl}, the inductance L_{cl} and the capacitance C_{cl}, during the forced commutation and the natural commutation (reverse recovery of the diode). While the losses of C_{cl} can be neglected, the losses of L_{cl} depend on the inductance design and the operating point of the converter. For these reasons these losses are not considered in the following.

Fig. 22 presents the losses of D_{cl} and R_{cl} during IGBT turn-on and turn-off transients at $Tj = 125\,°C$ and $V_{DC} = 2.5\,kV$. Both loss components have been determined by measurements.

The R_{cl} losses increase for rising L_{cl} due to the slower

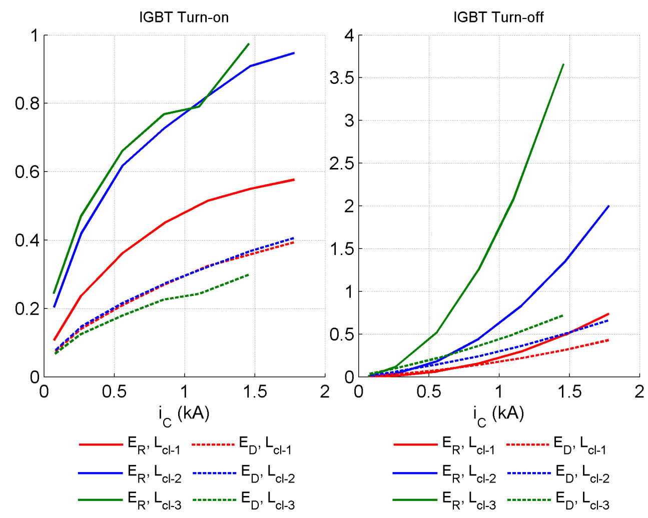

Fig. 22: Snubber losses as function of i_{C} current for different clamp configurations ($T\mathrm{j} = 125\,°\mathrm{C}$, $V_{\mathrm{DC}} = 2.5\,\mathrm{kV}$).

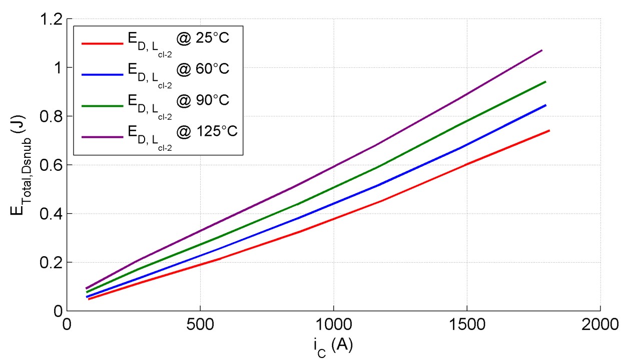

Fig. 23: Clamp diode losses at IGBT turn-on as function of collector current i_{C} with $T\mathrm{j}$ as parameter ($V_{\mathrm{DC}} = 2.5\,\mathrm{kV}$ and $L_{\text{cl-2}} = 2\,\mu\mathrm{H}$).

demagnetization. These losses dominate the clamp losses at IGBT turn-on and turn-off transients. The increase of L_{cl} reduces the losses in $\mathrm{D_{cl}}$ during IGBT turn-on transients, due to the smaller $\mathrm{d}i_{\mathrm{C}}/\mathrm{d}t$ and the reduced reverse recovery current. The rise of L_{cl} increases the losses in $\mathrm{D_{cl}}$ during IGBT turn-off transients (Fig. 22).

The clamp diode turn-off losses increase almost linear with the rising collector current between 0.39 mJ/A at 25 °C and 0.58 mJ/A at 125 °C. The losses at nominal current increase by about 35 % from 25 °C to 125 °C (0.46 J to 0.71 J) (Fig. 23).

The function of total losses of the clamp resistance and the device current is non linear. At nominal current the losses increase by about 10 % from 25 °C to 125 °C (1.49 J to 1.65 J) (Fig. 24). The total losses of the clamp resistance increase with rising L_{cl}, making the total losses at high currents for $L_{\text{cl-3}}$ larger than those at hard switching.

3) Total Losses E_{Total}: The sum of semiconductor and clamp component losses E_{Total} for the clamp configuration $L_{\text{cl-2}}$ can

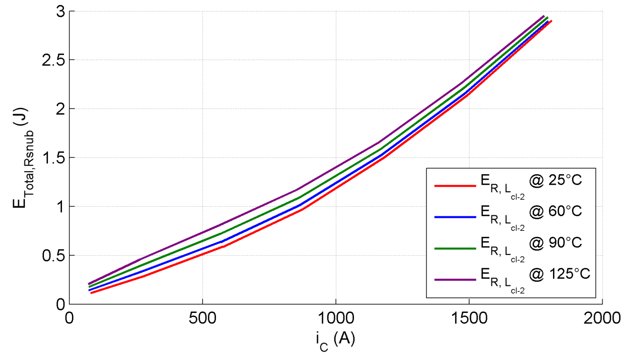

Fig. 24: Clamp resistance losses at IGBT turn-on as function of collector current i_{C} with $T\mathrm{j}$ as parameter ($V_{\mathrm{DC}} = 2.5\,\mathrm{kV}$ and $L_{\text{cl-2}} = 2\,\mu\mathrm{H}$).

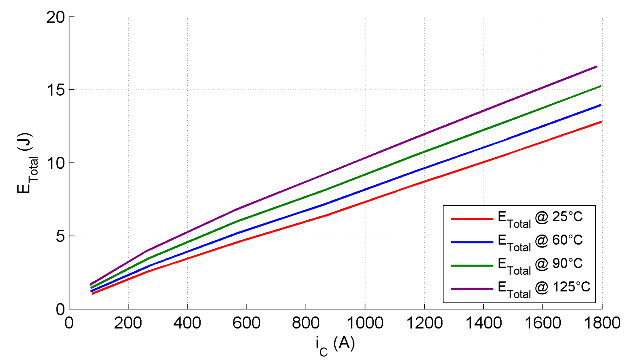

Fig. 25: Total switching losses as function of collector current i_{C} with $T\mathrm{j}$ as parameter ($V_{\mathrm{DC}} = 2.5\,\mathrm{kV}$ and $L_{\text{cl-2}} = 2\,\mu\mathrm{H}$).

be seen in Fig. 25. It is interesting that the losses $E_{\text{Total SC}}$ and E_{Total} are lower than those at hard switching in a current range between 600 to 1800 A at $V_{\mathrm{DC}} = 2.5\,\mathrm{kV}$. As expected, the total losses almost linearly increase with rising collector current.

The total losses for the nominal current increase by about 26 % from 25 °C to 125 °C (8.62 J to 11.63 J). Moreover, the total semiconductor losses increase by about 31 % from 25 °C to 125 °C (6.61 J to 9.49 J), which represents a loss reduction of about 30 to 20 % compared to the switching losses at hard switching, see Fig 25.

4) Comparison of Switching and Clamp Losses: The losses of semiconductors and clamp components are compared in Figs. 26 and 27 at $V_{\mathrm{DC}} = 2.5\,\mathrm{kV}$, $i_{\mathrm{C}} = 1.2\,\mathrm{kA}$, $T\mathrm{j} = 125$ and 25 °C.

The IGBT turn-on losses are reduced by 79 % for $L_{\text{cl-1}}$, 89 % for $L_{\text{cl-2}}$ and 92 % for $L_{\text{cl-3}}$ refered to hard switching (0.86 J for $L_{\text{cl-1}}$, 0.45 J for $L_{\text{cl-2}}$ and 0.33 J for $L_{\text{cl-3}}$ compared to 4.12 J for hard switching). The diode turn-off losses increase by 9.3 % for $L_{\text{cl-1}}$, 2 % for $L_{\text{cl-2}}$ and decrease by 10 % for $L_{\text{cl-3}}$ compared to hard switching (4.01 J for $L_{\text{cl-1}}$, 3.74 J for $L_{\text{cl-2}}$ and 3.3 J for $L_{\text{cl-3}}$ regarding the 3.67 J for hard switching). IGBT turn-off transients cause an increase of about 8 % for the configurations with clamp compared to hard switching.

The total semiconductor losses $E_{\text{Total SC}}$ at $T\mathrm{j} = 125\,°\mathrm{C}$ and

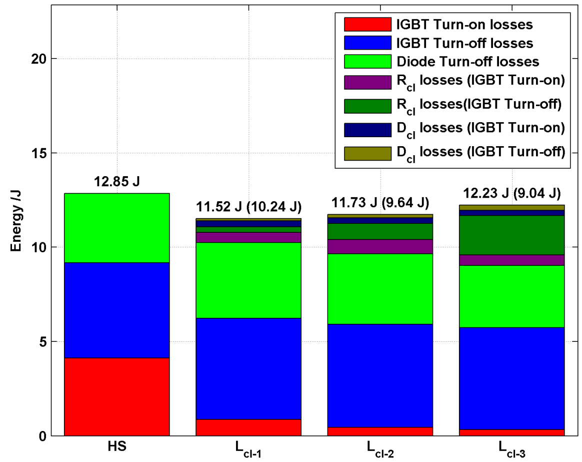

Fig. 26: Comparison of Switching and Clamp Losses for different configurations ($T\mathrm{j} = 125\,°\mathrm{C}$, $V_{\mathrm{DC}} = 2.5\,\mathrm{kV}$, $i_{\mathrm{C}} = 1.2\,\mathrm{kA}$).

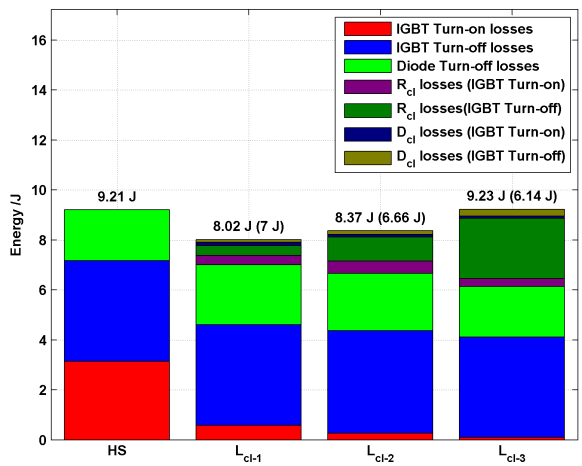

Fig. 27: Comparison of Switching and Clamp Losses for different configurations ($T\mathrm{j} = 25\,°\mathrm{C}$, $V_{\mathrm{DC}} = 2.5\,\mathrm{kV}$, $i_{\mathrm{C}} = 1.2\,\mathrm{kA}$).

nominal current $i_{\mathrm{C}} = 1.2\,\mathrm{kA}$ are reduced by 21 % for $L_{\text{cl-1}}$, 25 % for $L_{\text{cl-2}}$ and 30 % for $L_{\text{cl-3}}$ compared to hard switching (10.24 J for $L_{\text{cl-1}}$, 9.64 J for $L_{\text{cl-2}}$ and 9.04 J for $L_{\text{cl-3}}$, 12.85 J for hard switching).

Based on these results the clamp operation of the 4.5 kV press-pack IGBTs is an interesting technical solution which enables a higher silicon utilization due to reduced switching losses. Furthermore the clamp configuration reduces the stress during IGBT turn-on transients. A low value of L_{cl} increases the stress of the diode. The total converter losses are only slightly changed by the clamp configuration. The optimum value of L_{cl} depends on the required switching frequency of the application.

V. Conclusions

This paper characterizes the new 85 mm, 4.5 kV, 1.2 kA Westcode press-pack SPT+ IGBT in VSCs applying a clamp circuit which is used in IGCT VSCs today. The switching behavior of both IGBT and freewheeling diode are investigated for the first time for clamp configurations of varying load currents, junction temperatures and clamp inductances.

The experimental results show that the stress of IGBT and diode can be substantially reduced by the use of the clamp circuit. Furthermore IGBT turn-on losses and diode turn-off losses can be substantially reduced compared to hard switching (e.g. by 92 % and 10 % at 125 °C, $L_{\text{cl-3}}$ =5.6 µH, 1.2 kA). On the other hand the IGBT turn off losses slightly increase in clamp configurations compared to hard switching (e.g. at 125 °C, $L_{\text{cl-3}}$ =5.6 µH, 1.2 kA by about 8 %).

Compared to hard switching the total semiconductor losses $E_{\text{Total SC}}$ can be reduced by 30 %- 33 % at $L_{\text{cl-3}}$ =5.6 µH and by 21 %- 24 % at $L_{\text{cl-1}}$ =1 µH for $T\mathrm{j} = 125\,°\mathrm{C}$ and $T\mathrm{j} = 25\,°\mathrm{C}$ respectively.

However, the clamp circuit does not influence the converter efficiency substantially, since the saved switching losses are almost compensated by the additional clamp losses.

Nevertheless, the proposed circuit configuration is very attractive for Medium Voltage IGBT VSCs due to the increased silicon utilization. Thus higher converter currents and powers can be achieved using a given semiconductor. Obviously the attractiveness of clamp configurations increases for high switching frequency applications.

References

[1] S. Bernet, "State of the art and developments of medium voltage converters an overview," in *Proc. PELINCEC 2005*, Warsaw, Poland, 2005.

[2] J. Rodriguez, S. Bernet, B. Wu, J. Pontt, and S. Kouro, "Multilevel voltage-source-converter topologies for industrial medium-voltage drives," *IEEE Trans. on Industrial Electron.*, vol. 54, no. 6, pp. 2930–2945, Dec. 2007.

[3] S. Bernet, "Recent developments of high power converters for industry and traction applications," *IEEE Trans. on Power Electron.*, vol. 15, no. 6, pp. 1102–1117, Nov 2000.

[4] F. Wakeman and G. Lockwood, "Electromechanical evaluation of a bondless pressure contact igbt," *IEE Proceedings Circuits, Devices and Systems*, vol. 148, no. 2, pp. 89–93, Apr 2001.

[5] S. Bernet, "State-of-the-art and trends of high voltage power devices and medium voltage converters for industry and transportation," in *Proc. 5th International Workshop: Future of Electronic Power Processing and Conversion, IEEE-FEPPCON*, Salina, Italy, 2004.

[6] K. Fujii, P. Koellensperger, and R. De Doncker, "Characterization and comparison of high blocking voltage IGBTs and IEGTs under hard- and soft-switching conditions," *IEEE Trans. on Power Electron.*, vol. 23, no. 1, pp. 172–179, Jan. 2008.

[7] D. Linzen, J. von Bloh, and R. De Doncker, "Characterization of a high-voltage press pack IGBT under soft-switching conditions," *Conf. Rec. IEEE-IAS Annu. Meeting*, vol. 3, pp. 2170–2174 vol.3, 2002.

[8] M. Rahimo, A. Kopta, S. Eicher, U. Schlapbach, and S. Linder, "Switching-self-clamping-mode "SSCM", a breakthrough in SOA performance for high voltage IGBTs and diodes," in *Proc. Int. Symp. on Power Semiconductor Devices and ICs, ISPSD*, Kitakyushu, Japan, May 2004.

[9] M. Rahimo, A. Kopta, R. Schnell, U. Schlapbach, S. Zehringer, and S. Linder, "2.5kv-6.5kv industry standard IGBT modules setting a new benchmark in SOA capability," in *Proc. 25th International PCIM Conference*, Nuernberg, Germany, May 2004, pp. 314–319.

[10] R. Alvarez, F. Filsecker, and S. Bernet, "Characterization of a new 4.5 kv press pack spt+ igbt for medium voltage converters," in *Proc. 1st IEEE Energy Conversion Congress and Exposition*, San Jose, USA, 2009.

[11] T. Setz and M. Luescher, *Integrated Gate Commutated Thyristors Application Note, Applying IGCTs*. ABB Switzerland Ltd.: http://www.abb.com/semiconductors, 2006.

[12] S. Tschirley, B. S., and S. P., "Design and characteristics of reverse conducting 10-kv-igcts," in *Proc. od IEEE-Power Electronics Specialist Conference (PESC)*, Rhodos,Greece, June 2008.